Journal of Insect Physiology 120 (2020) 103995

Contents lists available at ScienceDirect

Journal of Insect Physiology

journal homepage: www.elsevier.com/locate/jinsphys

Fluid dynamics in the functional foregut of xylem-sap feeding insects: A comparative study of two *Xylella fastidiosa* vectors

Emanuele Ranieri[a,1], Gianluca Zitti[b,*,1], Paola Riolo[a], Nunzio Isidoro[a], Sara Ruschioni[a], Maurizio Brocchini[b], Rodrigo P.P. Almeida[c]

[a] Dipartimento di Scienze Agrarie, Alimentari e Ambientali – Università Politecnica delle Marche, Ancona, Italy
[b] Dipartimento Ingegneria Civile, Edile e dell'Architettura – Università Politecnica delle Marche, Ancona, Italy
[c] Department of Environmental Science, Policy and Management – University of California, Berkeley, Berkeley, CA, USA

ARTICLE INFO

Keywords:
Meadow spittlebug
Blue green sharpshooter
Precibarium
Micro computed tomography
Hydrodynamic model
CFD

ABSTRACT

Xylem sap sucking insects are adapted to ingest fluids under tension. Although much has been learned about such feeding strategy, this adaptation still poses several unresolved questions, including how these insects ingest against strong xylem sap tension. Xylem sap-feeding insects are vectors of the plant pathogenic xylem-limited bacterium *Xylella fastidiosa*. This bacterium colonizes the cuticular lining of the foregut of vectors in a persistent manner. We used micro-computed tomography and scanning electron microscopy to investigate the foregut morphometry of two *X. fastidiosa* vector species: *Philaenus spumarius* and *Graphocephala atropunctata* (Hemiptera: Aphrophoridae and Cicadellidae, respectively). On the basis of morphometric data, we built a hydrodynamic model of the foregut of these two insect species, focusing on the precibarium, a region previously shown to be colonized by *X. fastidiosa* and correlated with pathogen acquisition from and inoculation to plants. Our data show that space in the *P. spumarius* functional foregut could potentially harbor twice as many cells as similar space in *G. atropunctata*, although the opposite trend has been observed with biological samples. Average flow velocity of ingested fluid depended on the percentage of the cibarium volume exploited for suction: if the entire volume were used, velocities were in the range of meters per second. In contrast, velocities on the order of those found in the literature (about 10 cm/s) were attained if only 5% of the cibarium volume were exploited. Simulated bacterial colonization of the foregut was analyzed in relation to hydrodynamics and pressure needed for insects to ingest. Our model is designed to represent the diameter reduction of the food canal in both insect species when infected with *X. fastidiosa*. Results indicated that full bacterial colonization significantly increased the mean sap-sucking flow velocity. In particular, the colonization increased the maximum section-averaged velocity in the *G. atropunctata* more than two times and the net pressure needed to mantain the flow in the precibarium when colonized is relevant (about 0.151 MPa) if compared to a standard xylem sap tension (1 MPa). Bacterial colonization also influenced the sucking process of the *G. atropunctata*, by hindering the formation of a recirculation zone (or eddy), that characterizd the flow in the distal part of the precibarium when bacteria were absent. On the other hand, considering the pressure the insect must generate to feed, *X. fastidiosa* colonization probably influences fitness of the *G. atropunctata* more than that of *P. spumarius*.

1. Introduction

Xylem sap-feeders are insects adapted to obtain nourishment from an energetically costly and nutritionally dilute substrate (Raven, 1983). These insects have an efficient muscular pump, the cibarium, to suck plant sap under tension. The cibarium is located between the stylets and the esophagus, after which the anatomical foregut or alimentary canal proper starts. The food canal in the stylets are connected to the cibarium through a narrow channel: the precibarium, which is lined with chemosensory papillae separated into two groups by the precibarial valve (Backus and McLean, 1983). Because of the low nutrient content in xylem sap, these insects ingest a large amount of sap. They also generally excrete large volumes of liquid that may reach, in some species, up to 1,000 times their body mass in a 24 h period (Mittler, 1967; Horsfield, 1978). In other words, xylem sap ingestion is energetically expensive, but the mechanics and energy requirements to

* Corresponding author.
E-mail address: g.zitti@univpm.it (G. Zitti).
[1] Contributed equally to this work.

https://doi.org/10.1016/j.jinsphys.2019.103995
Received 2 May 2019; Received in revised form 28 November 2019; Accepted 8 December 2019
Available online 12 December 2019
0022-1910/

feed on such diet are yet to be understood.

Electrophysiology and electromyography studies have revealed that xylem sap-feeders have a complex feeding physiology. The rate of the cibarial muscle activity varies, with an average of 1.22 ± 0.05 Hz for the leafhopper *G. atropunctata* (Hemiptera: Cicadellidae) (Almeida and Backus, 2004) and 0.7 Hz for the spittlebug *Philaenus spumarius* (Hemiptera: Aphrophoridae) (Cornara et al., 2018). Cibarial muscle contraction period of 0.175–0.350 s was recorded for another leafhopper, *Homalodisca vitripennis* (Dugravot et al., 2008). During each cibarial muscle contraction event, sap fluid passes through the stylets and precibarium, entering the cibarial chamber. Muscle relaxation increases pressure in the chamber, resulting in sap being pushed into the midgut. Additionally, sap could move back to the stylets, through the precibarium; however, that movement does not occur due to the presence of a pressure sensitive check valve (precibarial valve), which blocks flow backwards (Ruschioni et al., 2019). The speed of sap flow into the mouthparts has been estimated to be ~7.8–8 cm/s in *G. atropunctata* (Purcell et al., 1979) to 30–50 cm/s in *H. vitripennis* (Andersen et al., 1992), estimates obtained by considering volumes excreted, dimensions of the food canal of these leafhopper species, and sap fluid behaving like water. In other words, available estimates assume that sap flow through the food canal occurs constantly over a period of time. However, from a simplified perspective, sap ingestion occurs at distinct, rhythmically repeating stages, namely fluid sucking from plants into the cibarial chamber, followed by pushing of that fluid into the midgut. Focusing on the actual sap flow in the precibarium, here we analyzed only the first of these two stages of ingestion.

Although the functional morphology of the foreguts of different xylem sap feeders has been studied (Raven, 1983; Backus and McLean, 1983), this particular feeding adaptation still poses a number of questions. First, in piercing the plant tissue with the stylets to feed on xylem, insects must avoid embolization/cavitation of the vessels so that ingestion can occur; the role of salivary sheaths to prevent cavitation during stylet penetration of vessels has been hypothesized (Backus and Lee, 2011; Crews et al., 1998), but remains enigmatic. Moreover, xylem sap is typically under considerable tension; the negative pressure may vary depending on plant site, time of day, and plant condition, and it is often measured down to −3 MPa (Pockman et al., 1995; Kim, 2013). Ingestion in this condition requires the generation of strong pressures, but how these insects generate such pressures is not yet understood. These species have large cibarial muscles and a structurally reinforced precibarium (Backus, 1985; Malone et al., 1999); such morphological adaptations would be compatible with requirements to suck against such tensions (Malone et al., 1999; Novotny and Wilson, 1997). Nevertheless, the maximum tension that muscles can generate has been proposed to be on the order of 0.1 MPa (Raven, 1983; Kim, 2013; Young and Schmidt-Nielsen, 1985). Yet feeding ratios (function of xylem sap nutritional components and tension) of these insects support a capability to pump against −1.8 MPa (Andersen et al., 1992).

The discrepancy among these observations is intriguing. Numerical techniques, based on physical models and boundary conditions derived or deduced from measurement, represent a more precise way to use the measured data, and could help to better understand the observations. Detailed knowledge on the feeding mechanism of xylem sap-sucking insects is also of applied importance because all these species are vectors of the xylem-limited plant pathogenic bacterium *Xylella fastidiosa* (Sicard et al., 2018), and the development of hydrodynamic models of vector foreguts could be critical in future studies on vector-pathogen interactions. This bacterium has a unique feature among pathogens spread by arthropods. It multiplies in the insect foregut without being circulative in the hemolymph (Almeida et al., 2005). The retention sites in vectors are localized in the precibarium and the cibarium (Almeida and Purcell, 2006; Purcell et al., 1979; Brlansky et al., 1983), but the impacts of bacterial colonization on insect feeding, fitness, and how bacterial inoculation of plants occurs remain to be determined.

The spittlebug *P. spumarius* and the leafhopper *G. atropunctata* are important vectors of *X. fastidiosa* in Europe and California, USA, respectively. The biology of *X. fastidiosa* transmission by these insects is similar, despite the fact that they belong to different families (Cornara et al., 2016). There are few estimates of *X. fastidiosa* populations on the cuticular surface of the cibarium and precibarium of insect vectors, but recent studies with *P. spumarius* indicate that cell populations are reasonably small, with $10^2 - 10^3$cells per insect (Cornara et al., 2016; Saponari et al., 2014). On the other hand, populations in *G. atropunctata* may be small during early stages of colonization, but normally reach ~10^4cells per insect (Retchless et al., 2014; Labroussaa et al., 2017). The role of different fluid dynamics in the foregut has been hypothesized as a possible explanation (Cornara et al., 2016). Another relevant factor is the role of bacterial colonization on vector fitness. Scanning electron microscopy (SEM) observations of colonized individuals of both insect species reveal the presence of large biofilms on the precibarium (Almeida and Purcell, 2006; Brlansky et al., 1983; Alves et al., 2008), compatible with the assumption that sap-sucking would be negatively impacted by reductions in lumen diameter in that canal. Interestingly, *X. fastidiosa* cells form a colony of polarly attached cells on the surface of insect vectors (e.g. Almeida and Purcell, 2006; Brlansky et al., 1983; Newman et al., 2004). Whether acquisition of bacteria by insects leads to fitness reduction also remains to be determined.

We propose that sap fluid dynamics in the foregut of insect vectors may explain some of these biological observations, help understand how *X. fastidiosa* colonizes vectors, and the potential impacts of these interactions on vector feeding and acquisition/inoculation of *X. fastidiosa*. To test our hypothesis we compared the morphometry and geometry of the precibarium profiles of *P. spumarius* and *G. atropunctata*. Photographs of the two insects are reported in Fig. 1.

On the basis of the micro-computed tomography (μCT) reconstructions of the precibarium profiles of these vector species, we developed two hydrodynamic models per insect: i) one not colonized by *X. fastidiosa* (NC); and another ii) with full *X. fastidiosa* cell colonization (C), represented by a bacterial biofilm covering the length of the precibarium. We focused on the fluid dynamics associated with sap intake through the precibarium, as that region has been correlated with *X. fastidiosa* inoculation to plants (Almeida and Purcell, 2006). While limited in scope, the analyses of these models provide novel insights on these interactions; future experimental and quantitative work will be needed to incorporate other components of the system such as sap tension in the plant host as well as insect operation of valves and fluid movement into the midgut.

2. Materials and methods

2.1. Insects

Philaenus spumarius and *G. atropunctata* adults used in the experiments were obtained from the University of California's greenhouses in Berkeley, from rearing colonies established from individuals collected from field populations in Alameda and Sonoma counties, Northern California. General methods and protocols as for maintaining insects were as previously described (e.g. Cornara et al., 2016; Zeilinger et al.,

Fig. 1. A photograph of a P. spumarius (right panel) and some *G. atropunctata* (left panel). Credits to Dylan Beal, UCB.

2018). Morphometric data was generated using measurements from μCT and SEM samples. While μCT provided three-dimensional information, SEM was used to generate relative standard deviation for all the measurements obtained throught μCT (see Table S2 in the Supporting information).

2.2. μCT sample preparation

Freshly collected adults were anesthetized by exposure to low temperatures (−18 °C) for 60 s, then immediately immersed into a solution of glutaraldehyde and paraformaldehyde 2.5% in 0.1 M cacodylate buffer +5% sucrose, pH 7.2–7.3 and left at 4 °C overnight. The specimens were then post-fixed in 1% OsO_4(osmium tetroxide) for 1.5 h at room temperature and rinsed in 0.1 M cacodylate buffer. Dehydration in a graded ethanol series from 35% to 99%, was followed by critical point drying.

2.3. μCT images acquisition, reconstruction and analysis

Fixed specimens of both species mantained at University of California, Berkeley were analyzed using a SkyScan1272 at the MicroPhotonics facility (Micro Photonics Inc. Allentown, PA). The beam energy was set to 50 keV in a current source of 20 0 μA. The image pixel size resolution was 1.999,974 μm and pictures were captured over a global 360° rotation sampled at steps of 0.1°. Surface area and linear measurements acquisition was carried out in ImageJ binarizing the tomograms by setting a grey-level threshold (Max Entropy method), above which voxels (volume-pixels) were taken as part of the insect and below which voxels were taken as part of the background. Additional linear measurements of the different tomograms were performed through DataViewer V1.5.2.4.

2.4. Scanning electron microscopy (SEM)

Thirty-one adult individuals per species of both sexes were used for the observations. Insects were anaesthetized by exposure to cold temperatures (−18 °C) for 60 s, then stored in 60% alcohol at 4 °C until sample processing. Individuals were dissected by removing the head capsule from the rest of the body. Specimens were dehydrated in a series of graded ethanol, from 60% to 99%, 15 min each. After ethanol dehydration, samples were critical point dried and stored within a desiccator until observed with an SEM. On each aluminum stub, 5 samples were mounted. The observations were carried out using a Hitachi® TM-1000 SEM.

2.5. Morphometrical analysis

For an accurate reconstruction of the foregut, each 2 μm resolution μCT tomogram was analyzed by means of surface area, perimeter, and average diameter. In this analysis, the precibarial valve, located at the junction of the distal and proximal sections of the precibarium, was assumed to be in the open position, given that the study only considered the dynamics of sap flow into the precibarium, and not events past this stage during ingestion. The number of cells of *X. fastidiosa* potentially hosted in the precibarium of both species was calculated considering that (in condition of high degree of colonization) the cuticle may host 6.7 cells/μm^2, based on measurements of SEM images of insect colonization of mouthparts of *G. atropunctata*, obtained from Almeida and Purcell (2006) (see Fig. S1 in the Supporting information). To estimate the impact of *X. fastidiosa* colonization on the diameter of the lumen of the precibarium, each cell was considered to occupy the volume of a cylinder with 0.3 μm of diameter and 2.2 μm of linear length (Wells et al., 1987). The cibarium chamber was taken as an ellipsoid, whose volume calculation was based on use of its 3 perpendicular axes of symmetry. Relative Standard Deviation (RSD) was calculated on the basis of SEM observations on 31 specimens (both male and female individuals) of *P. spumarius* and 31 specimens of *G. atropunctata* (Table S2; Fig. S2).

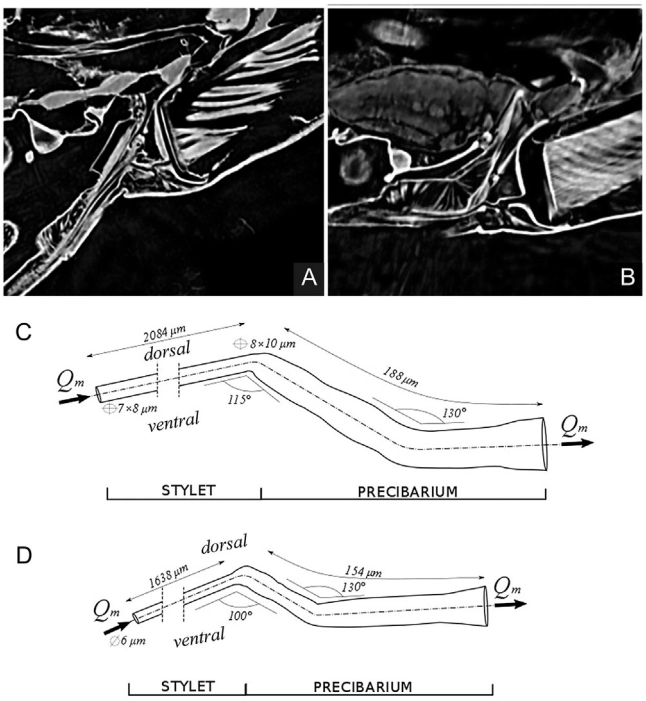

Fig. 2. General description of the foregut morphology of *P. spumarius* and *G. atropunctata*. A) *Philaenus spumarius* tomogram took on the sagittal plane showing the cibarium (Ci), the precibarium (Pr) and the stylets (St). B) *Graphocephala atropunctata* tomogram taken on the sagittal plane showing the cibarium (Ci), the precibarium (Pr) and the stylets (St). C) Schematic drawing showing the fundamental dimensions and geometry of *P. spumarius* Pr and St. D) Schematic drawing showing the fundamental dimensions and geometry of *G. atropunctata* Pr and St. The complicated bending geometry of the precibarium reported in the tomograms (A, B) are simplified in the schematic drawings (C, D), where the axis of the food channel are taken to be straight lines bending twice: at the edge between the precibarium and the stylet food canal, and in the middle of its length.

2.6. Computational fluid dynamic simulations

The geometries of the precibarium for both *P. spumarius* and *G. atropunctata*, obtained with the methods described above, were used to simulate the flow inside the precibarium and in a proximal section of the food canal in the stylets by means of the Computational Fluid Dynamics (CFD) Software Ansys© Fluent. While this study focused on the precibarium, only a portion of the scanned food canal in the stylets (250 μm for the *P. spumarius* and 150 μm for the *G. atropunctata*) was included in the simulation, with the aim of reproducing correctly the fluid flow entering the precibarium. The total length of the stylets (see Fig. 2C, D and Table S1) was not reproduced in the simulations, since it would entail a relevant computational cost. This simplification is valid because the fluid dynamics in vessels is driven by pressure gradients and not by absolute pressures (see e.g. Poiseuille law, frequently used in literature: Andersen et al., 1992; Novotny and Wilson, 1997; Loudon and McCulloh, 1999). Part of the stylets were maintained to reproduce the effects of curvature at the connection beween the stylet and the precibarium. A three-dimensional domain of these parts was designed with a CAD software, assuming the precibarium to be a cylinder with circular section, characterized by a variable radius. Radius variations correspond to the measures of the morphometrical analysis. The axis of the cylinder was taken to be a straight line that bends twice: at the edge between the precibarium and the stylet food canal, and in the middle of its length (Fig. 2). As shown in Fig. 2A, B, precibarium has a complex

bending geometry. Our simplification enabled use of a simple model for both species, which is based on the assumption that small curvatures have negligible effects on the fluid dynamics. Hence, the only two largest curves are reproduced, using the measured angles. A curvilinear coordinate was used, increasing from the inlet section along the central axis of the numerical domain. Sketches of both domains, with the main geometrical information, are reported in Fig. 2C, D. The geometry of the precibarium, fully colonized by *X. fastidiosa* was estimated reducing the radius of the precibarium by 2.2 μm, equal to the reported linear length of the bacterium (Wells et al., 1987). We assumed that *X. fastidiosa* cells were polarly attached to the cuticle of insects, as previously observed in several studies (e.g. Almeida and Purcell, 2006; Brlansky et al., 1983; Newman et al., 2004).

The geometry considered for the two insects was used to simulate the suction flow with CFD. CFD solved the fluid dynamics by dividing the domain in simpler and smaller elements (cells), and evaluating the fluid dynamic variables (pressures and velocities) at a finite number of points (nodes). In our simulation the domain is divided in cells with tetrahedral shape. The maximum edge size of the cells was 0.75 μm in the precibarium and 1 μm in the stylet food canal. This produced a mesh of 793,689 cells and 797,660 nodes for *P. spumarius* and a mesh of 110,297 cells and 117,912 nodes for *G. atropunctata* in the not colonized configuration, and a mesh of 533,923 cells and 543,390 nodes for *P. spumarius* and a mesh of 351,148 cells and 66,653 nodes for *G. atropunctata* in the colonized configuration. A pressure-based numerical model was used, which solved for a water (density $\rho = 1000$ kg m^{-3} and dynamic viscosity $\mu = 1.003 \cdot 10^{-3}$ kg m^{-1} s^{-1}) flow in the laminar regime. More details on the laminar-turbulent regime are discussed below, when the Reynolds number is introduced.

The numerical simulations reproduced the mass flow during ingestion. Hence, simulations did not reproduce the beginning and end phases of the suction, but only the full speed flow in a quasi-steady regime. Such regime is achieved when the flow does not vary in time, being the pressure gradient along the food channel fixed. The flow was forced to satisfy the following boundary conditions: no slip condition along the walls of the precibarium, mass inflow at the distal section of the stylet food canal and mass outflow at the proximal section of the precibarium. The mass inflow and outflow were evaluated using the cibarium volumes, estimated with the morphometrical analysis. The true volume used for the suction (i.e. the cibarium volume) is unknown, therefore a parametric analysis was performed using four percentages of the total volume of the cibarium, i.e. 5%, 20%, 50% and 100%. The time needed to fill such volumes was assumed to be of 0.75 s (Dugravot et al., 2008), such estimated rate being the only one available in literature. Considering the largest food channel diameter evaluated from the morphometry (see Table 2 in the section RESULTS), the suction time and the water kinematic viscosity, the Womersley number is $Wo \ll 1$ and confirms the assumption of a quasi-steady flow (see also Loudon and Tordesillas, 1998). The flow discharge was estimated by dividing the volume ingested (i.e. the cibarium exploited volume) by the time interval during which it was ingested. The mass flow evaluated with different volume percentages for *P. spumarius* and *G. atropunctata* are reported in Table 1. The pressure at the inflow boundary condition has been conventionally assigned equal to −1 MPa, which is compatible with typical xylem sap tensions. Also, the reference pressure at the inflow affected the result only in relation to absolute pressures, not pressure gradients or velocities. In fact, the flow in our model is triggered by imposing a mass outflow (estimated using results from laboratory measurements) at the boundary of the geometry corresponding to the cibarium entrance.

Table 1
Table of flow rates $Q_m$evaluated for different percentage of cibarium volume exploited for the suction in *P. spumarius* (Ps) and *G. atropunctata* (Ga).

Cibarium Volume Exploited	Q_m Ps (10^{-7}kgs s^{-1})	Q_m Ga (10^{-7} kg s^{-1})
100%	2.051	1.160
50%	1.025	0.580
20%	0.410	0.232
5%	0.103	0.058

For the simulations, the regime of the flow is assumed to be laminar. In particular, the laminar flow is characterized by smooth paths of the fluid particles, without lateral mixing, eddies or swirls of fluids. An estimate of the flow regime is given through the Reynolds number *Re*and laminar regimes in pipes are characterized by $Re < 2000$. The magnitudes of the Reynolds number in the precibarium have been estimated at section Ω of average diameter D_m, using as reference velocity scale $U_m$the maximum section-averaged velocity $Q_m/\rho\Omega$:

$$Re = \frac{(Q_m/\rho\Omega)D_m}{\mu/\rho} \quad (1)$$

The maximum value of *Re*is given by the maximum section-averaged velocity, which corresponds to the maximum flow rate, i.e. to an exploitation of 100% of the cibarium volume for the suction (see Table 1). Considering the average diameter of the precibarium, it was found $Re = 16.22$ for *P. spumarius* and $Re = 14.90$ for *G. atropunctata*, while diameter reduction due to colonization led to $Re = 18.78$ for the *P. spumarius* and $Re = 19.14$ for the *G. atropunctata*. These small values of the maximum possible *Re*, justify the assumption of laminar flow, which has been used in the numerical solution. The quasi-steady assumption was also verified with a transient (time-dependent) numerical simulation, reproducing the flow in the domain for a duration of 0.75 s, with time steps of 0.001 s. The results of the transient simulation showed no time dependence. Our CFD simulations were characterized by a relative error of 10^{-5} for the mass conservation (continuity equation) and 10^{-7} for the momentum conservation, i.e. velocities.

Obviously, the simulated conditions are simplifications: the effects due to bacterial colonization occur before complete colonization, and bacterial colonization may lead to an increase in muscle effort, reducing the percentage of exploited cibarium volume and subsequently a flow velocity reduction in place of the net pressure rise. However, the model provides realistic information on the impact that the food canal diameter reduction (due to colonization) could have on the ingestion fluid dynamics for both insects. We also note that we assume that all precibarial surfaces are colonized by *X. fastidiosa*; however that is not the case in nature. Soon after pathogen acquisition *X. fastidiosa* colonization of vectors is patchy (Almeida and Purcell, 2006); however, with longer periods, extensive colonization of the precibarial canal has been observed, with the exception of the area associated with the precibarial valve (e.g. Newman et al., 2004, Fig. 4B). It is possible that spatial patterns observed in the abovementioned studies are not universal, as those focused on *G. atropunctata* and not other species.

3. Results

3.1. Foregut profile

The precibarium (Pr) is a narrow canal, starting from the hypopharyngeal extension, which inserts into the food canal formed by the stylets (St), and ends in the cibarial chamber (Ci) (Fig. 2A, B). μCT and SEM observation reveal that the precibial profile of both species is generally narrow in the distal part (also termed the D-sensillum field; Backus and Morgan, 2011) while it enlarges quickly in the proximal half (also termed the epipharyngeal basin and precibarial trough; Backus and Morgan, 2011), until it connects with the cibarium (Fig. 2C, D; Ci). The precibarium bends once in dorsal direction, in the middle of its longitudinal axis, with an angle of ~130°. The bend corresponds to the location of the precibarial valve, on the epipharygeal side (lower side in Fig. 2 drawings). Morphometric data of the two species, generated using measurements from μCT, are presented in Table 2. According to SEM observations, relative standard deviations of ±6.9% for

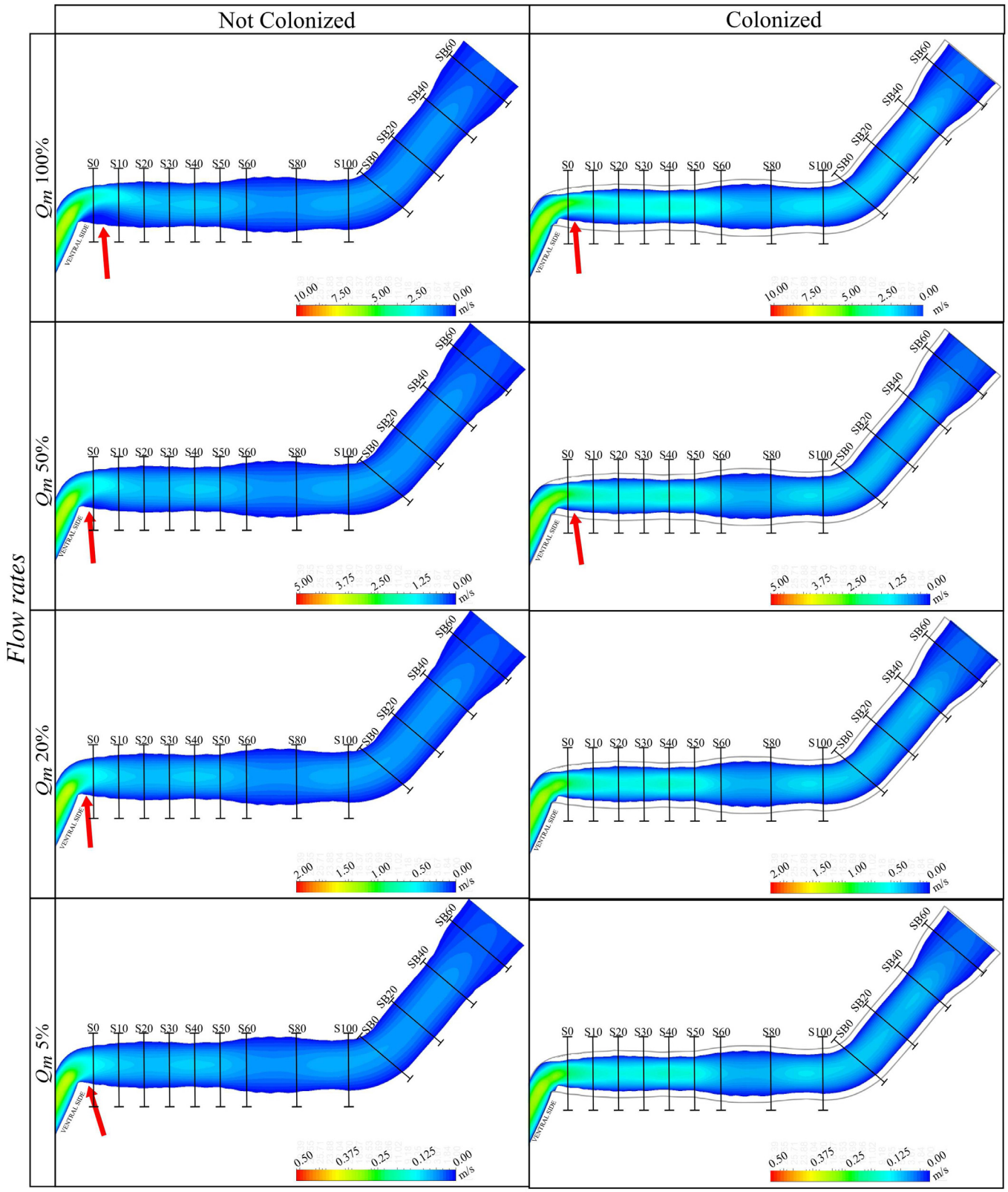

Fig. 3. Velocity map of the longitudinal streamwise section of the precibarium, from the stylets to the cibarium edge, representing the hydrodynamics of the xylem sap flow in the precibarium of the *P. spumarius* during ingestion in the not colonized (left panels) and colonized (right panels) conditions, for the four different flow rates, corresponding to different percentages of exploited cibarium volume. Colour scale represents the estimated velocity. The eddies are indicated with red arrows. (For interpretation of the references to colour in this figure legend, the reader is referred to the web version of this article.)

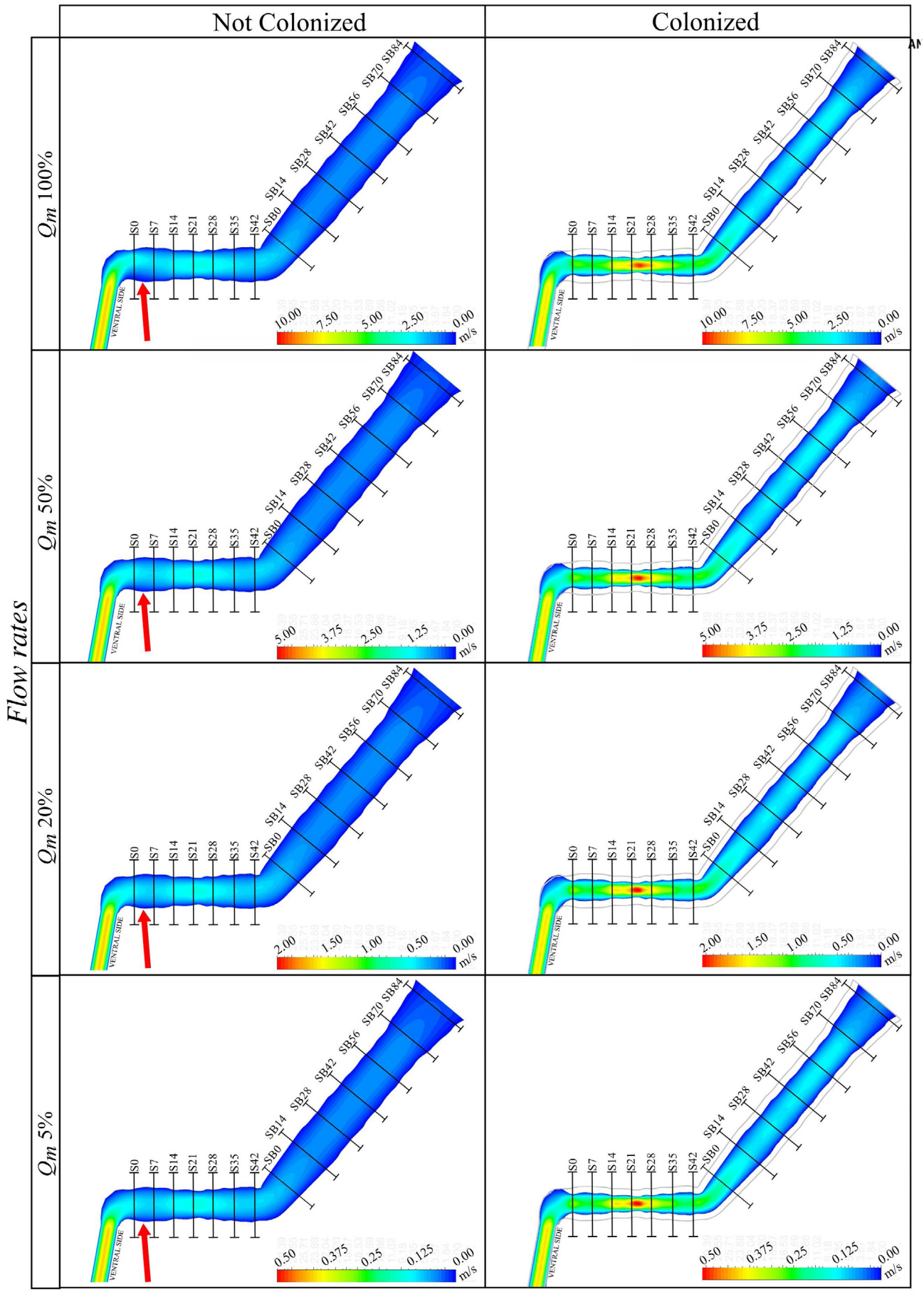

(caption on next page)

Fig. 4. Velocity map of the longitudinal streamwise section of the precibarium, from the stylets to the cibarium edge, representing the hydrodynamics of the xylem sap flow in the precibarium of the *Graphocephala atropunctata* during ingestion in the not colonized (left panel) and colonized (right panel) conditions, for the four different flow rates, corresponding to different percentages of exploited cibarium volume. Colour scale represents the estimated velocity. The eddies are indicated with red arrows. (For interpretation of the references to colour in this figure legend, the reader is referred to the web version of this article.)

P. spumarius and of ±5.1% for *G. atropunctata*, were calculated for all the values in Table 2.

3.2. Flow in precibarium

Computational Fluid Dynamic (CFD) simulation in the 3D reconstructed model provided a detailed description of the fluid dynamics in the two insect foreguts, in both configurations (fully colonized by *X. fastidiosa* and free from other bacteria). Velocity maps on the longitudinal section for the four different flow rates are reported in Figs. 3 and 4 for *P. spumarius* and *G. atropunctata*, respectively, where the clean conditions, i.e. not colonized, are illustrated in the left panels and the colonized conditions in the right panels. For a more detailed comparison of the velocity variation along the precibarium, transversal sections were sampled along the precibarium part of the domain, perpendicularly to its axis. The first section was located at the boundary with the stylets and the subsequent sections were located downstream with intervals of 20 μm for *P. spumarius* and 14 μm for *G. atropunctata*. A refinement was performed in a portion of the precibarium, halving the spacing between sections, because of the more complex flow expected in this area. The location of these sections along the full length of the precibarium has been reported in the images of Fig. 3 for *P. spumarius* (from S0 to SB60) and Fig. 4 for *G. atropunctata* (from S0 to SB84). Sections labelled as S refer to the distal part of the precibarium (near to the stylet fascicle) while sections labelled as SB are located in the proximal part (near to the cibarium). For each sampled section, the maximum velocity (v_{max}), the minimum velocity (v_{min}) and section-averaged velocity (v_{av}) were evaluated and reported in Table S3. The space variation of the section-averaged velocity downstream for each flow rate and for each section diameter is shown in Fig. 5 (in the top panels for *G. atropunctata* and in the bottom panels for *P. spumarius*). The space variation of the maximum and minimum velocities downstream are available in Figs. S3 and S4.

Although the morphometry and geometry of the precibarium profile of these two insects were different, the flow characteristics of the clean conditions in the two domains were similar. For both insects the flow velocity fell in the same range, which varied with the flow rate. If 100% of the cibarium volume were exploited, the maximum velocity would reach values of 2.9–3.5 m s^{-1}. The highest velocities (8.2 m s^{-1}) were estimated in the food canal leading to the precibarium, due to its smaller diameter. For 50% of cibarium volume exploited, the maximum velocity reached 1.5 m s^{-1}, for 20% of volume exploited, was 0.5 m $s^{-1}$and for 5% of volume exploited was 0.12–0.15 m s^{-1}, i.e. comparable in size to the values typically found in the literature. For the largest flow rate (100% of the cibarium volume exploited), some negative (i.e opposite to the flow direction) velocities occurred, near a portion of zero mean velocity. These zero and negative velocities are due to the formation of an eddy, that makes the fluid recirculate in the portion of the food canal where it occured. This eddy is located ventrally, between sections S0 and S30, with an approximate length of 20 μm for *P. spumarius* (see Fig. 3) and between sections S0 and S14, with an approximate length of 15 μm for *G. atropunctata* (see Fig. 4). For smaller flow rates (20% and 5% of the cibarium volume exploited) such eddy gradually decreased.

When the condition was of full colonization, the velocity in the precibarium in the two insects displayed large differences. The velocity became higher in both insects, but larger peaks are evident for the *G. atropunctata*. For example, if 50% of the cibarium volume were exploited, the maximum velocity in the *P. spumarius* increased from 1.37 m $s^{-1}$to 2.42 m s^{-1}, while in the *G. atropunctata* the maximum velocity increased from 1.47 m $s^{-1}$to 4.57 m $s^{-1}$and occurred more downstream. Moreover, the eddy located ventrally, gradually disappeared for smaller flow rate for the fully colonized *P. spumarius*, while it was completely absent in the fully colonized *G. atropunctata*.

The section-averaged pressure $p_{av}$was evaluated in the sampled

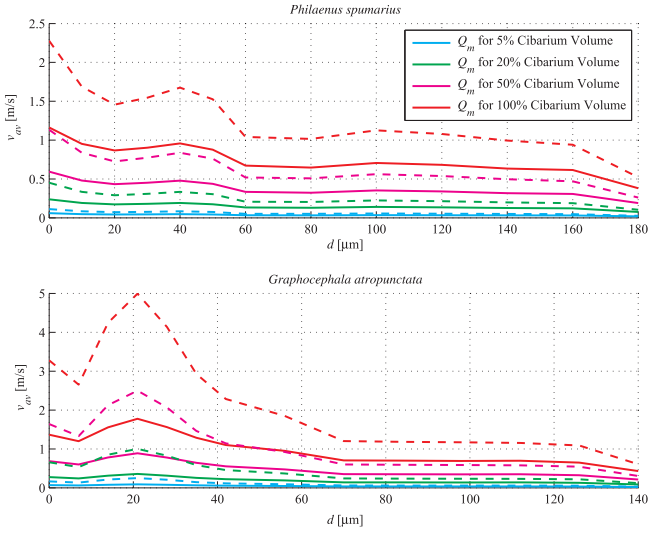

Fig. 5. Variation of the sectio-averaged velocity in the sections sampled along the curvilinear coordinate of the precibarium (*d*) for *P. spumarius* (top panel) and *G. atropunctata* (bottom panel), in the not colonized (solid line) and colonized (dashed line) conditions.

Table 2
Table of *P. spumarius* (Ps) and *G. atropunctata* (Ga) foregut morphometry. Pr = Precibarium; Di = distal half of Pr; Pm = proximal half of Pr. Pr sections in first column are ordered from the distal to the proximal one. Measurement procedure provided resolution was 2 μm, but intervals of 16 μm are reported for space limitation.

Pr sections	Ps (μm^2)	Ga (μm^2)
Pr 0 μm	152	100
Pr 16 μm	240	108
Pr 32 μm	264	72
Pr 48 μm	244	120
Pr 64 μm	336	143
Pr 96 μm	300	196
Pr 112 μm	329	188
Pr 128 μm	342	192
Pr 152 μm	348	300
Foregut dimensions		
cibarium volume (mm^3)	0.154	0.087
stylets mean area (μm^2)	52.5[a]	28
stylets length (μm)	2080[b]	1640(b)
precibarium volume (μm^3)	52600	20,200
mean area Di (μm^2)	283	99.4
mean diameter Di (μm)	19.00	11.25
mean area Pm (μm^2)	470	221
mean diameter Pm (μm)	24.5	16.8
Xylella fastidiosa cells potentially hosted in Pr	66,700	36,200
Overall dimensions		
body length (mm)	~5.5	~5

[a] see Malone et al. (1999).
[b] is considered to protrude up to 1 mm to reach the xylem (Malone et al., 1999)

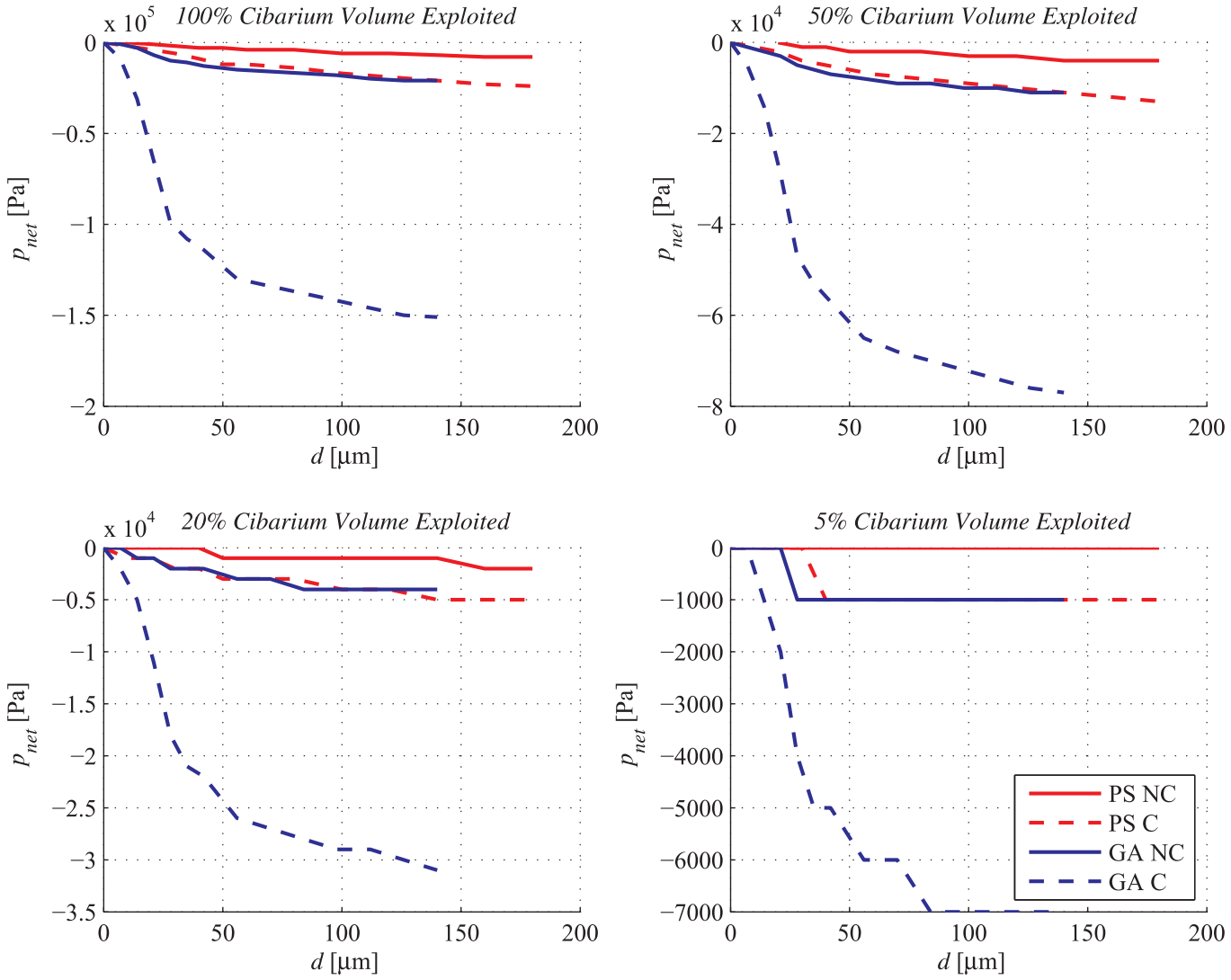

Fig. 6. Variation of the net pressure along the curvilinear coordinate of the precibarium *d*(distance from the stylet edge) for *P. spumarius* (grey lines) and *G. atropunctata* (black lines) in the not colonized (solid lines) and colonized (dashed lines) condition, for different flow rates, corresponding to different cibarium volume exploitation.

Table 3
Table of the net pressure in the last section of the precibarium $p_{net,f}$(in the colonized (C) and not colonized (NC) condition) and pressure gradient growth due to colonization evaluated for different percentage of the cibarium volume exploited for the suction in *P. spumarius* and *Graphocephala atropunctata*.

Cibarium	*P. spumarius*			*G. atropunctata*		
Volume Exploited	$p_{net,f,NC}$ [Pa]	$p_{net,f,C}$ [Pa]	Δp^* [%]	$p_{net,f,NC}$ [Pa]	$p_{net,f,C}$ [Pa]	Δp^* [%]
100%	−8000	−24,000	200%	−21,000	−151,000	619%
50%	−4000	−13,000	225%	−11,000	−77,000	600%
20%	−2000	−5000	150%	−4000	−31,000	675%
5%	–	−1000	–	−1000	−7000	600%

sections. The flow in the food channel does not depend on the absolute pressure, but on the pressure gradient, i.e. the difference in pressure per unit length along the food channel (as stated by the Hagen-Poiseuille law, Loudon and McCulloh, 1999). Hence, the net pressure $p_{net}$is defined, by removing from the section-averaged pressure at each section the section-averaged pressure at the entrance of the precibarium, i.e. at the section S0:

$$p_{net} = p_{av} - p_{av}(S0) \quad (2)$$

The net section-averaged pressure, evaluated like this, represented the pressure variation along the curvilinear coordinate of the precibarium and is reported in Fig. 6 for *P. spumarius* and *G. atropunctata* in the not colonized and colonized conditions (see Table S3, including the actual section-averaged pressures). The net pressure at the last section close to the cibarium increased with colonization. For example, if 50% of the cibarium volume was exploited, for *P. spumarius* the net pressure at the last section was − 4000 Pa for the clean condition and − 13, 000 Pa for the colonized condition, while for *G. atropunctata* it was − 11, 000 Pa for the clean condition and − 77, 000 Pa for the colonized condition. Then, the pressure gradient the insect had to exert to maintain the flow in the precibarium food channel increased 2 times for *P. spumarius* and 6 times for *G. atropunctata*. The percentage of growth in pressure gradient along the precibarium, reported in Table 3 for each different condition, was evaluated with the ratio:

$$\Delta p^* = \frac{p_{net,f,C} - p_{net,f,NC}}{p_{net,f,NC}} \quad (3)$$

where $p_{net,f,NC}$ was net pressure at the last section in the not colonized condition and $p_{net,f,C}$ was the net pressure at the last section in the colonized condition. The results of the simulation reproducing the flow

in the *P. spumarius* functional foregut for a 5% use of the cibarium volume are not reported since the net pressure in the not colonized condition was too low (lower than the numerical model precision).

4. Discussion

The detailed morphometry and the numerical simulations provided a description of the fluid dynamics that occurs in the precibarial canal of the functional foregut of the studied insects. Our analysis of the fluid dynamics provide new details on the flow of ingested sap, assuming that no cavitation occurs, that sap behaves like water, and that the precibarium is evenly tubular. The assumptions on the sap tension at the inflow and on the length of the stylets prevented the model from generating reliable results on the absolute pressure in the precibarium. Nevertheless, the net pressure in the precibarium was evaluated to understand the precibarium contribution to the sap tension, especially when colonized. For clean conditions, the net pressure was found to be small in comparison to the xylem sap tension: it was $|p_{net}| < 0.025$ MPa for the maximum flow rate (100% of the cibarium volume exploited) and $|p_{net}| < 0.001$ MPa for the minimum flow rate (5% of the cibarium volume exploited). Therefore, the precibarium has a negligible effect on the tension the insect must generate to ingest if it is not colonized. On the other hand, results showed a complex velocity pattern in the precibarium when colonization occurs, and such fluid dynamics may be of biological relevance.

Research involving *X. fastidiosa* and its vectors have increased dramatically in recent years (Almeida, 2016), but many unsolved questions remain. *Xylella fastidiosa* attaches to, and in adult insects persistently colonizes, the cuticular lining of the foregut of insect vectors (Purcell et al., 1979). Our series of morphometric comparisons between *P. spumarius* and *G. atropunctata*, indicate that *P. spumarius* could potentially harbor twice as many cells as *G. atropunctata*, because the surface area of the precibarial chamber is approximately twice as large in *P. spumarius*. However, the population size in *G. atropunctata* was found larger than in *P. spumarius*. This suggests that the bacterial population size discrepancy observed in these two vectors is not due to different cuticular surface available for colonization in their foreguts, but probably to a combination of other factors related to the fluid dynamics in the insect mouthparts and potentially surface chemistry.

The section-averaged velocity of the intake sap in the foreguts of both examined species, estimated with our numerical model, are strictly related to the percentage of the cibarium volume exploited for the suction and can reach very large values (up to 5 m s^{-1}, if 100% of the cibarium volume was exploited). Values previously reported in literature, i.e. Purcell et al. (1979) and Andersen et al. (1992), for the speed of ingested sap were of the order of centimeters per second. In particular, Purcell et al. (1979) provided the value of 0.08 m s^{-1}. In our study similar section-averaged velocities were found if only 5% of the cibarium volume was exploited and ranged from 0.02 to 0.06 m s^{-1} for the *P. spumarius* and from 0.02 to 0.09 m s^{-1} for the *G. atropunctata*. These computed velocities are based on accurate anatomical data, measured with high resolution non-destructive techniques, and on the only data available for the cibarium muscle pumping time, which is 0.75 s (Dugravot et al., 2008). Therefore, we deduced that either the percentage of the cibarium operative for the pumping is very small (about 5%) or the velocities suggested in the literature underestimated the actual fluid velocity in the precibarium. When bacteria are absent, the eddy in the ventral side of the distal precibarium is evident for the larger discharges: it occupies almost half of the canal if 100% of the cibarium volume is exploited, while it is negligible if only 5% of the cibarium volume is exploited.

The analysis of the model with full bacterial colonization revealed that, because of the different anatomical dimensions of the two vectors, the effects of *X. fastidiosa* presence are distinctly different for each. The reduction of the food canal diameter increased the section-averaged velocities, which reached 0.12 m s^{-1} in *P. spumarius* and 0.25 m s^{-1} in *G. atropunctata* (values corresponding to the 5% of the cibarium volume exploited). Such velocity increase was expected (stated by basic fluid mechanical principles). However the three dimensional numerical model reproduced the major geometrical characteristics of the studied insects, such as the diameter variation and the main bending of the precibarium, and was able to simulate accurately the fluid dynamics (e.g. the presence of eddies). Comparing the two species, *G. atropunctata* is subjected to the largest colonization effects in terms of velocity variation (see high velocity zones evident in the distal part of the colonized precibarium; red area in Fig. 4).

Still, *X. fastidiosa* colonization affects the hydrodynamics in the distal part of the precibarium, where the recirculation area (eddy) disappears in both insect species. Only in *P. spumarius*, for the largest dicharges (50% and 100% of the cibarium volume exploited) the eddy was present also with colonization, even if its size is reduced. Such data suggest that the presence of the bacteria has a larger impact on the *G. atropunctata* dynamics than on those of *P. spumarius*. This difference in behaviour could be due to the wider diameter of the food canal in *P. spumarius* vs *G. atropunctata*. On the other hand, the relatively long length of the distal precibarium in the *P. spumarius* should not affect the eddy formation, since the size of the eddy is significantly smaller than the length of the precibarium in both insect species. The presence of these eddies, i.e. low velocity recirculating zones, could be of great importance for the deposition and infection of the bacteria. However, the size of the eddy in the *P. spumarius* is bigger than that in *G. atropunctata*, and this does not justify the larger colonization in *G. atropunctata* compared *P. spumarius*.

The increase in energy required for vectors to ingest when colonized with *X. fastidiosa* can be estimated through the differences in net pressure, representing the resistence to sap flow, given by the precibarium with a reduced food canal lumen. We observed that a large contribution to the net pressure occurred in the distal part of the precibarium of both species. Once again, that region of precibarium appears to be a bottleneck for ingestion compared to the middle or proximal areas (towards the cibarium). Insect fitness should be impacted by this additional energy requirement. In particular, the total net pressure is of potential importance for the colonized condition of *G. atropunctata*. In fact, we observed the most significant increase in pressure gradient for this vector. The total net pressure developed in the *G. atropunctata* precibarium reaches values of $|p_{net}| = 0.151$ MPa for the maximum flow rate (100% of the cibarium volume exploited) and of $|p_{net}| = 0.007$ MPa for the smaller flow rate (5% of the cibarium volume exploited). In the former case the net pressure developed in the *G. atropunctata* precibarium represents an important contribution to the tension that muscles must generate to feed, compared with typical xylem sap tension. Instead, the net pressures developed in the *P. spumarius* were significantly smaller, being $|p_{net}| = 0.024$ MPa for the maximum flow rate and of $|p_{net}| = 0.001$ MPa for the smallest flow rate. This suggests that the precibarium colonization could have a significant influence on the fitness of *G. atropunctata*, but minor influence on *P. spumarius*. Even if the simulated conditions are simplifications, the fitness of these insects under field conditions would be similarly impacted by the reduction of volume of sap ingested, or the longer suction period, to obtain the same amount of fluid. These results also suggest that *P. spumarius* may tolerate precibarium colonization conditions better than *G. atropunctata*.

In conclusion, the present study investigates, for the first time, the hydrodynamics in the foregut of sap-sucking species by means of a numerical 3D model, built on accurate morphometric data. This model can be the basis for other investigations on mechanisms of xylem sap feeding and *X. fastidiosa* transmission; future experimental and quantitative work will provide more accurate characterization of xylem sap in the plant host and of cibarial pumping. Currently, neither the measured surface available for colonization, nor the hydrodynamics of ingested sap, explain the differences in *X. fastidiosa* populations reported in *P. spumarius* and *G. atropunctata*. Finally, the consequences of the full

colonization of *X. fastidiosa* in the precibarium of the two vector species were evaluated in terms of differences in speed, dynamics and in pressure necessary to feed. Additional electrophysiology and model-based simulation studies are needed to better understand the physiology of xylem sap feeders and *X. fastidiosa* transmission mechanisms.

Future studies in relation to impacts of *X. fastidiosa* colonization on insect fitness are difficult to propose: we have attempted in the past, and continue today, to experimentally test if bacterial colonization impacts leafhopper/spittlebug fitness. However, these experiments have proven to be very challenging to perform. On the other hand, future studies on the fluid mechanics of the processes of interest could focus on the role of the wall boundary conditions to be used. Some evidence suggests that a slip-boundary condition would be more suited than the no-slip condition. Hence, dedicated studies could span from analytical investigations of the slip model by parametrically changing the slip lengths, vessel radius, volume discharges, etc. Further, the role of the rheology in use for the sap fluid would be of interest and would require dedicated laboratory experiments and new numerical simulations.

Data availability

The μCT Images mentioned in section Materials and Methods, limited to the head of the two insects discussed in this paper, are available as images in jpg format at the linkhttps://figshare.com/s/f023261da7c354fdd990,https://doi.org/10.6084/m9.figshare.7322165.

CRediT authorship contribution statement

Emanuele Ranieri: Conceptualization, Methodology, Validation, Formal analysis, Investigation, Data curation, Writing - original draft, Writing - review & editing. **Gianluca Zitti:** Conceptualization, Methodology, Validation, Formal analysis, Investigation, Data curation, Writing - original draft, Writing - review & editing. **Paola Riolo:** Writing - review & editing, Supervision. **Nunzio Isidoro:** Writing - review & editing, Supervision. **Sara Ruschioni:** Writing - review & editing. **Maurizio Brocchini:** Conceptualization, Resources, Writing - review & editing, Supervision. **Rodrigo P.P. Almeida:** Conceptualization, Resources, Writing - review & editing, Supervision, Project administration, Funding acquisition.

Acknowledgments

We acknowledge Brandon Walters from Micro Photonics for his support and help in µCT software analysis. We also acknowledge Guangwei Min and Reena Zalpuri (University of California Berkeley Electron Microscopy Facility) for assistance with microscopy. The research was funded by the California Department of Food and Agriculture PD/GWSS Research Program. We thank E.A. Backus (USDA Agricultural Research Service, Parlier, CA, USA), C. Loudon (University of California, Irvine, CA, USA), and one anonymous reviewer for helpful comments that improved this manuscript.

Appendix A. Supplementary data

Supplementary data associated with this article can be found, in the online version, at https://doi.org/10.1016/j.jinsphys.2019.103995.

References

Almeida, R.P., 2016. Xylella Fastidiosa vector transmission biology. In: Vector-Mediated Transmission of Plant Pathogens. APS Press St Paul, Minnesota, USA. pp. 165–174.
Almeida, R.P., Backus, E.A., 2004. Stylet penetration behaviors of graphocephala atropunctata (Signoret) (hemiptera, cicadellidae): EPG waveform characterization and quantification. Ann. Entomol. Soc. Am. 97 (4), 838–851.
Almeida, R.P., Blua, M.J., Lopes, J.R., Purcell, A.H., 2005. Vector transmission of Xylella Fastidiosa: applying fundamental knowledge to generate disease management strategies. Ann. Entomol. Soc. Am. 98 (6), 775–786.
Almeida, R.P., Purcell, A.H., 2006. Patterns of Xylella Fastidiosa colonization on the precibarium of sharpshooter vectors relative to transmission to plants. Ann. Entomol. Soc. Am. 99 (5), 884–890.
Alves, E., Leite, B., Marucci, R.C., Pascholati, S.F., Lopes, J.R., Andersen, P.C., 2008. Retention sites for Xylella Fastidiosa in four sharpshooter vectors (Hemiptera: Cicadellidae) analyzed by scanning electron microscopy. Curr. Microbiol. 56 (5), 531–538.
Andersen, P.C., Brodbeck, B.V., Mizell III, R.F., 1992. Feeding by the leafhopper, Homalodisca Coagulata, in relation to xylem fluid chemistry and tension. J. Insect Physiol. 38 (8), 611–622.
Backus, E., et al., 1985. Anatomical and sensory mechanisms of leafhopper and planthopper feeding behavior. Leafhoppers Planthoppers 163–194.
Backus, E.A., Lee, W.K., 2011. Glassy-winged sharpshooter feeding does not cause air embolisms in the xylem of well-watered plants. In: Esser, T. (Ed.), Proc. Pierce's Dis. Res. Symp. California Department of Food and Agriculture, Sacramento, pp. 3–7.
Backus, E.A., McLean, D.L., 1983. The sensory systems and feeding behavior of leafhoppers. II. A comparison of the sensillar morphologies of several species (Homoptera: Cicadellidae). J. Morphol. 176 (1), 3–14.
Backus, E.A., Morgan, D.J.W., Aug 2011. Spatiotemporal colonization of Xylella Fastidiosa in its vector supports the role of egestion in the inoculation mechanism of foregut-borne plant pathogens. Phytopathology 101 (8), 912–922.
Brlansky, R., Timmer, L., French, W., McCoy, R., 1983. Colonization of the sharpshooter vector, Oncometopia Nigricans and Homalodisca Coagulata by xylem-limited bacteria. Phytopathology 73 (4), 530–535.
Cornara, D., Garzo, E., Morente, M., Moreno, A., Alba-Tercedor, J., Fereres, A., Jul 2018. EPG combined with micro-CT and video recording reveals new insights on the feeding behavior of philaenus spumarius. PLoS One 13 (7), e0199154.
Cornara, D., Sicard, A., Zeilinger, A.R., Porcelli, F., Purcell, A.H., Almeida, R.P.P., 2016. Transmission of Xylella Fastidiosa to grapevine by the meadow spittlebug. Phytopathology 106 (11), 1285–1290.
Crews, L.J., McCully, M.E., Canny, M.J., Huang, C.X., Ling, L.E.C., Apr 1998. Xylem feeding by spittlebug nymphs: some observations by optical and cryo-scanning electron microscopy. Am. J. Bot. 85 (4), 449–460.
Dugravot, S., Backus, E.A., Reardon, B.J., Miller, T.A., Dec 2008. Correlations of cibarial muscle activities of Homalodisca spp. sharpshooters (Hemiptera: Cicadellidae) with EPG ingestion waveform and excretion. J. Insect Physiol. 54 (12), 1467–1478.
Horsfield, D., Jul 1978. Evidence for xilem feeding by Philaenus Spumarius (l.) (Homoptera: Cercopidae). Entomol. Exp. Appl. 24 (1), 95–99.
Kim, W., sep 2013. Mechanics of xylem sap drinking. Biomed. Eng. Lett. 3 (3), 144–148.
Labroussaa, F., Ionescu, M., Zeilinger, A.R., Lindow, S.E., Almeida, R.P.P., Apr 2017. A chitinase is required for Xylella Fastidiosa colonization of its insect and plant hosts. Microbiology 163 (4), 502–509.
Loudon, C., McCulloh, K., 1999. Application of the Hagen-Poiseuille equation to fluid feeding through short tubes. Ann. Entomol. Soc. Am. 92 (1), 153–158.
Loudon, C., Tordesillas, A., 1998. The use of the dimensionless Womersley number to characterize the unsteady nature of internal flow. J. Theor. Biol. 191 (1), 63–78.
Malone, M., Watson, R., Pritchard, J., 1999. The spittlebug Philaenus Spumarius feeds from mature xylem at the full hydraulic tension of the transpiration stream. New Phytol. 143 (2), 261–271.
Mittler, T.E., 1967. Water tensions in plants – an entomological approach1. Ann. Entomol. Soc. Am. 60 (5), 1074–1076.
Newman, K.L., Almeida, R.P.P., Purcell, A.H., Lindow, S.E., 2004. Cell-cell signaling controls Xylella Fastidiosa interactions with both insects and plants. Proc. Natl. Acad. Sci. 101 (6), 1737–1742.
Novotny, V., Wilson, M.R., Jul 1997. Why are there no small species among xylem-sucking insects? Evol. Ecol. 11 (4), 419–437.
Pockman, W.T., Sperry, J.S., O'Leary, J.W., 1995. Sustained and significant negative water pressure in xylem. Nature 378 (6558), 715–716.
Purcell, A.H., Finlay, A.H., MCLean, D.L., 1979. Pierces disease bacterium: mechanism of transmission by leafhopper vectors. Science 206 (4420), 839–841.
Raven, J., 1983. Phytophages of xylem and phloem: a comparison of animal and plant sap-feeders. In: Advances in Ecological Research, vol. 13. Elsevier, pp. 135–234.
Retchless, A.C., Labroussaa, F., Shapiro, L., Stenger, D.C., Lindow, S.E., Almeida, R.P.P., 2014. Genomic insights into Xylella Fastidiosa interactions with plant and insect hosts. In: Genomics of Plant-Associated Bacteria. Springer, Berlin Heidelberg, pp. 177–202.
Ruschioni, S., Ranieri, E., Riolo, P., Romani, R., Almeida, R.P., Isidoro, N., 2019. Functional anatomy of the precibarial valve in Philaenus Spumarius (l.). PLoS One 14 (2), e0213318.
Saponari, M., Loconsole, G., Cornara, D., Yokomi, R., Stradis, A., Boscia, D., Bosco, D., Martelli, G., Krugner, R., Porcelli, F., 2014. Infectivity and transmission of Xylella Fastidiosa by Philaenus Spumarius (Hemiptera: Aphrophoridae) in apulia, italy. J. Econ. Entomol. 107 (4), 1316–1319.
Sicard, A., Zeilinger, A.R., Vanhove, M., Schartel, T.E., Beal, D.J., Daugherty, M.P., Almeida, R.P., 2018. Xylella Fastidiosa: insights into an emerging plant pathogen. Annu. Rev. Phytopathol. 56 (1), 181–202.
Wells, J.M., Raju, B.C., Hung, H.-Y., Weisburg, W.G., Mandelco-Paul, L., Brenner, D.J., Apr 1987. Xylella Fastidiosa gen. nov., sp. nov: gram-negative, xylem-limited, fastidious plant bacteria related to xanthomonas spp. Int. J. Syst. Bacteriol. 37 (2), 136–143.
Young, S.R., Schmidt-Nielsen, K., 1985. Animal physiology: adaptation and environment. J. Appl. Ecol. 22 (1), 291.
Zeilinger, A.R., Turek, D., Cornara, D., Sicard, A., Lindow, S.E., Almeida, R.P.P., 2018. Bayesian vector transmission model detects conflicting interactions from transgenic disease-resistant grapevines. Ecosphere 9 (11), e02494.